RSC Advances

PAPER

View Article Online
View Journal | View Issue

Cite this: *RSC Adv.*, 2018, **8**, 6904

A coumarin Schiff's base two-photon fluorescent probe for hypochlorite in living cells and zebrafish†

Kangnan Wang,[ab] Pengzhen Sun,[c] Xijuan Chao,[b] Duxia Cao,*[a] Zongwan Mao*[b] and Zhiqiang Liu*[d]

Received 4th January 2018
Accepted 31st January 2018

DOI: 10.1039/c8ra00093j

rsc.li/rsc-advances

Selective and sensitive fluorescent probes for ClO^- are desirable due to the importance of ClO^- in biological processes. Here, a coumarin Schiff's base, compound **1**, has been developed and successfully used as a one- and two-photon fluorescent probe for ClO^- with high selectivity. This probe can recognize ClO^- with obvious color change from yellow-green to colorless and green to blue fluorescence emission, which can be observed by the naked eye. The properties of low cytotoxicity and good cell permeability allow it to be used for ClO^- detection in living cells and zebrafish by both one- and two-photon microscopy imaging. All these results indicate that the compound is a sensitive probe with potential for analysis of ClO^- in biological samples. The mechanism by which probe **1** recognizes ClO^- is possibly nucleophilic addition followed by hydrolysis.

Introduction

Hypochlorite (ClO^-) is an important reactive oxygen species (ROS, mainly including H_2O_2, $OH^\bullet$, $^1O_2$, NO_2^-, HClO/ClO^- and so on),[1,2] which is biologically produced from chloride ions and hydrogen peroxide by the catalytic action of the enzyme myeloperoxidase (MPO) in living organisms.[3,4] Hypochlorite is a powerful oxidant and plays a critical role in the immune system against inflammation and microorganisms.[5,6] However, excessive intake of ClO^- may lead to tissue damage and diseases, such as lung injury, cancers and so on.[7–9] In addition, disinfected water with residual chlorine may cause organisms to suffer from diseases of the blood circulation and nervous system and irritation of sensory organs.[10,11] Therefore, detecting hypochlorite in drinking water and organisms is especially significant and attracts extensive interest.

Presently, there are a lot of methods available for hypochlorite determination, such as chemiluminescence and fluorescence methods and electroanalysis.[12] Among them, fluorescence titration is one of the most attractive methods owing to its high selectivity and sensitivity, real-time detection and easy processing.[13–16] Recently, many fluorescent probes for hypochlorite have been developed,[6,17–24] most of which are based on one-photon microscopy (OPM). The short excitation wavelength used in OPM may easily damage cells and tissues and lead to photobleaching, thus limiting the applications in tissues and living cells. Compared with OPM, two-photon fluorescence microscopy (TPM) normally uses longer excitation wavelength, which enables deep tissue imaging with focused excitation and reduces photobleaching and photodamage to biosamples.[25–27]

The numbers of selective ClO^- fluorescent probes are still limited. And most of the fluorescent probes still have some limitations, such as time dependence, poor selectivity, or complicated synthesis and rigorous conditions. Therefore, simple, fast, convenient fluorescent probes for ClO^- are still in high demand. Herein, a coumarin Schiff's base, compound **1**, was developed as a two-photon fluorescence probe for ClO^-. This water-soluble coumarin Schiff's base-based fluorescent probe, which can be obtained by simple synthesis under mild reaction conditions, has high fluorescence quantum yield and can detect ClO^- with high selectivity, rapid response rate and obvious color and fluorescence change, which can be observed by the naked eye. The probe is also successfully applied to imaging in living cells and living zebrafish by one- and two-photon modes.

Results and discussion

Spectroscopic recognition properties

Probe **1** was synthesized *via* the condensation reaction between 7-diethylaminocoumarin-3-aldehyde and 2-thiophenecarboxylic acid hydrazide according to a previously published method.[28] Probe **1** exhibits obvious UV-vis absorption and fluorescence recognition for ClO^-. Fig. 1a shows the change in UV-vis absorption spectrum of probe **1** to ClO^- in phosphate buffer/MeOH (6 : 4, v/v) solution. The absorption spectrum of probe

[a]School of Materials Science and Engineering, University of Jinan, Jinan 250022, PR China. E-mail: duxiacao@ujn.edu.cn

[b]MOE Key Laboratory of Bioinorganic and Synthetic Chemistry, School of Chemistry and Chemical Engineering, Sun Yat-sen University, Guangzhou 510275, PR China. E-mail: cesmzw@mail.sysu.edu.cn

[c]School of Pharmacy, Guangdong Pharmaceutical University, Guangzhou 510006, PR China

[d]State Key Laboratory of Crystal Materials, Shandong University, Jinan 250100, Shandong, PR China. E-mail: zqliu@sdu.edu.cn

† Electronic supplementary information (ESI) available. See DOI: 10.1039/c8ra00093j

1 showed a main absorption band at 455 nm ($\varepsilon = 5.02 \times 10^4\ M^{-1}\ cm^{-1}$) and a minor band at 317 nm ($\varepsilon = 1.09 \times 10^4\ M^{-1}\ cm^{-1}$). Upon titration with NaOCl, which was used as a source of ClO^-, the absorption band at 450 nm gradually decreased and showed a blue-shift to 373 nm with an isosbestic point at 339 nm. At the same time, the peak at 317 nm also decreased. These spectral changes indicate that a new compound was generated. The color change from yellow-green to colorless allows the colorimetric detection of ClO^- using the naked eye, and is invoked by a large blue-shift of *ca.* 80 nm in the absorption spectrum.

As expected, the emission profiles of probe **1** correlate to those of the absorption profiles in the presence of ClO^-. In the absence of ClO^-, probe **1** emits strong green fluorescence at 518 nm with fluorescence quantum yield of 0.27. Upon the addition of increasing concentrations of ClO^-, the fluorescence intensity decreases significantly upon excitation at 455 nm. This fluorescence decrease is caused by selective oxidation by ClO^-. As shown in Fig. 1b, a new fluorescence emission peak at 495 nm can be readily observed, and the fluorescence color changes from green to blue under UV light can also be clearly detected by the naked eye (Fig. 1b). This demonstrates that probe **1** is capable of sensing ClO^- efficiently in aqueous solution, acting as a ratiometric fluorescent probe.

One of the major challenges in ClO^- detection is to develop highly selective probes. In order to evaluate the selectivity of probe **1** toward ClO^-, possible influences caused by other analytes were investigated based on fluorescence spectra of solutions. The common anions and biologically related species ClO_4^-, $C_2O_4^{2-}$, NO_2^-, F^-, Cl^-, I^-, HCO_3^-, H_2O_2, CO_3^{2-}, NH_4^+, HSO_3^-, NO_3^-, Cys, OH^-, $S_2O_8^{2-}$, $S_2O_3^-$, SO_3^{2-}, SO_4^{2-}, GSH, HPO_4^{2-}, citric acid, boric acid and CH_3COO^- were used together with ClO^- to investigate the selectivity and competitiveness. As shown in Fig. S1,† among the ions tested, there were no obvious fluorescence changes observed except with ClO^-, and fluorescence change from green to blue was obviously observed only with addition of ClO^-. It is worth noting that other anions (up to 200 equiv.) did not interact with the probe and also did not interfere with the recognition for ClO^-. The results demonstrate the high selectivity of the probe for ClO^-.

To further examine the sensing mechanism of probe **1** for ClO^-, *in situ* electrospray ionization-mass spectroscopy (ESI-MS) was used to clarify the process of reaction between probe **1** and ClO^- (Fig. S2†). The mass spectrum peak of probe **1** is at 392.43 ($(M + Na)^+$). After the addition of ClO^-, there are two new mass peaks. A plausible mechanism by which probe **1** reacts with ClO^- according to ESI-MS data and ref. 14 and 29 is presented in Fig. 2. The new mass spectrum peaks at 426.34 and 284.30 may correspond to $(\mathbf{S\text{-}1} + Na)^+$ and $(\mathbf{P\text{-}1} + Na)^+$. The C=N bond is blocked, which leads to the decrease of the main absorption band at 455 nm and quenching of green fluorescence at 518 nm. Blue fluorescence emission after the addition of ClO^- may be derived from **P-1**.

Cytotoxicity and bioimaging of the probe

The need for a probe able to selectively detect ClO^- in living cells has recently attracted much attention because of the importance of ClO^- in biological applications. Therefore, probe **1** was applied to cells to demonstrate its potential application in cellular imaging. The cytotoxicity of probe **1** was evaluated by methyl thiazolyl tetrazolium (MTT) assay with probe concentration ranging from 0 μM to 50 μM (Fig. S3†). The experimental results indicate that the viability remains above 80% after 48 h incubation with different concentrations (0 μM to 50 μM) of probe **1**, indicating low cytotoxicity of probe **1**. Then cellular uptake of probe **1** in A549 cells was investigated. A549 cells were incubated with probe **1** at three distinct concentrations (10 μM, 20 μM, 50 μM) for 30 min. Strong green fluorescence in cells was observed by not only one-photon microscopy imaging ($\lambda_{ex} = 458$ nm) but also two-photon microscopy imaging ($\lambda_{ex} = 810$ nm) (Fig. 3). The short incubation time (30 min, Fig. S4†) with cells indicates quite good cell permeability of the probe. Thus low cytotoxicity and good cell membrane penetration make it applicable for detection of ClO^- in living cells.

Next the mechanism of cellular uptake of the probe was studied. As known, cells can take up small molecules by different

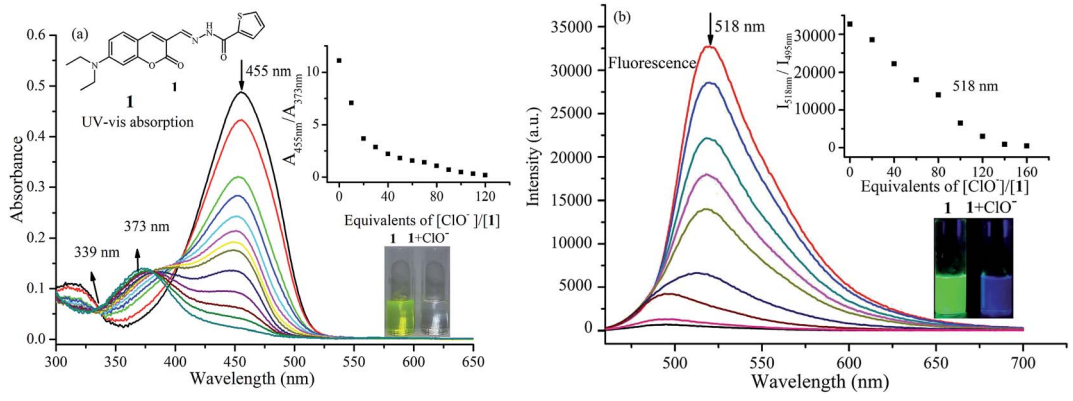

Fig. 1 Changes in UV-vis absorption (a) and fluorescence spectrum ($\lambda_{ex} = 450$ nm, (b) of probe **1** (10 μM)) with various amounts of ClO^- in potassium phosphate buffer (pH 7.4, containing 40% CH_3OH as co-solvent). The insets show ratios of absorbance at 455 nm and 373 nm (a) or fluorescence at 518 nm and 495 nm (b) as a function of ClO^- concentration, and color changes before and after the addition of ClO^- under natural light (a) and UV lamp (b).

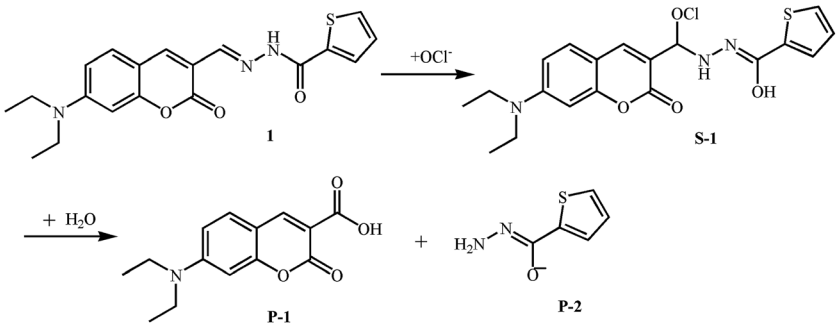

Fig. 2 A plausible mechanism by which probe **1** reacts with ClO^-.

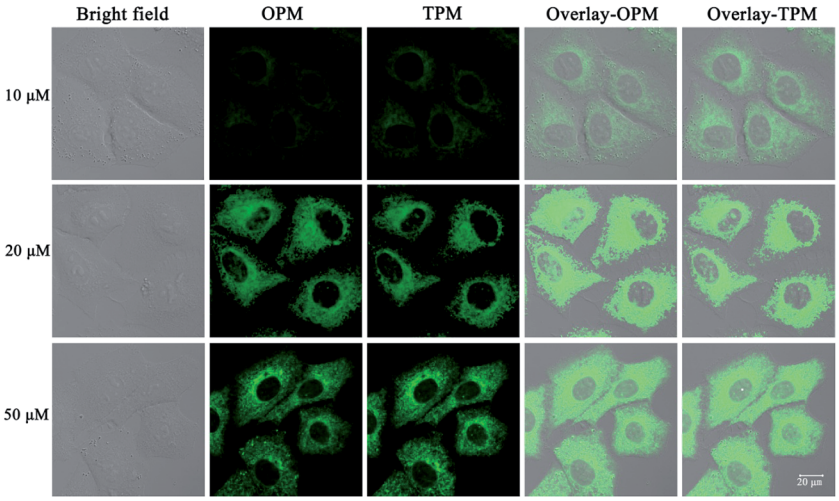

Fig. 3 One- and two-photon microscopy (OPM, TPM) confocal fluorescence images of A549 cells after incubation with probe **1** (10 μM, 20 μM and 50 μM) for 30 min and excitation at 458 nm (OPM) or 810 nm (TPM). The emission was collected at 520 ± 30 nm. Overlay-OPM: overlay of the bright field and OPM columns. Overlay-TPM: overlay of the bright field and TPM columns.

mechanisms.[30,31] Some mechanisms such as endocytosis and active transport mechanisms are energy-dependent. But some mechanisms such as facilitated diffusion and passive diffusion are energy-independent. First, temperature-dependence experiments were conducted. A549 cells (pre-placed at the respective temperatures for 30 min) were treated with probe **1** and incubated at different temperatures (37 °C, 25 °C and 4 °C) for 30 min. As shown in Fig. 4, at the lowest temperature, 4 °C, the images are not obvious and the images gradually become apparent as the temperature is increased, which indicates that lower temperature can reduce cellular uptake efficiency and thus cellular uptake is energy-dependent. In addition, treatments with two endocytosis modulators chloroquine and NH_4Cl, which can inhibit the acidification of endosomes and thus inhibit uptake by endocytosis, have no effect on the cellular uptake of probe **1**, which indicates endocytosis is not responsible for the cellular uptake. Taken together, these results indicate that probe **1** enters A549 cells possibly through an energy-dependent but non-endocytotic pathway.

Fluorescence detection of ClO^- in living cells

After establishing that the probe was capable of fluorescence detection of ClO^- and had good cellular uptake behavior, experiments to demonstrate the potential practical applications of the probe for fluorescence detection of ClO^- in living cells were performed. A549 cells were firstly incubated with probe **1** (20 μM) for 30 min; a strong green fluorescence was observed by both one-photon and two-photon excitation (Fig. 5A). After the cells were further incubated with 120 equiv. ClO^-, the cell images were recorded for a time series gradient. From Fig. S6,† we can see that green fluorescence in living cells was completely quenched after 25 min. If the cells were incubated with 10 equiv. (Fig. 5B) or 60 equiv. (Fig. 5C) ClO^-, the one-photon or two-photon fluorescence diminished gradually. When 120 equiv. ClO^- (Fig. 5D) was added, both one-photon fluorescence and two-photon fluorescence were completely quenched. Taken together, these results indicate that the probe can be successfully applied for one-photon and two-photon imaging of ClO^- selectively in living cells.

Fluorescence detection of ClO^- in zebrafish

To further examine whether ClO^- can be *in vivo* detected by probe **1**, 2 days-old zebrafish larvae were used as a vertebrate model. As shown in Fig. 6, bright emitted signals were clearly observed in all of the body of the zebrafish. When incubated with 20 μM probe **1** for 30 min, the zebrafish shows strong

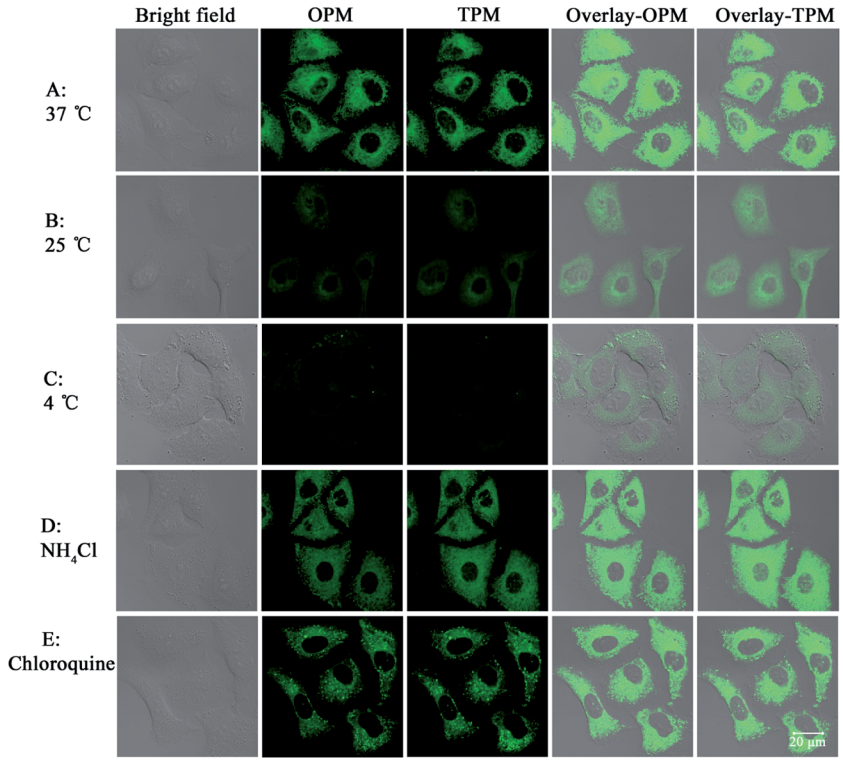

Fig. 4 Confocal images of A549 cells incubated with **1** (20 μM) under different conditions. (A)–(C): cells were incubated with **1** at 37 °C (A), 25 °C (B) or 4 °C (C) for 30 min. (D) and (E): cells were preincubated with NH_4Cl (50 μM) or chloroquine (10 μM) for 1 h at 37 °C and then incubated with **1** (20 μM) for 30 min, respectively. The probe was excited at 458 nm (OPM) or 810 nm (TPM). The emission was collected at 520 ± 30 nm. Overlay-OPM: overlay of the bright field and OPM columns. Overlay-TPM: overlay of the bright field and TPM columns.

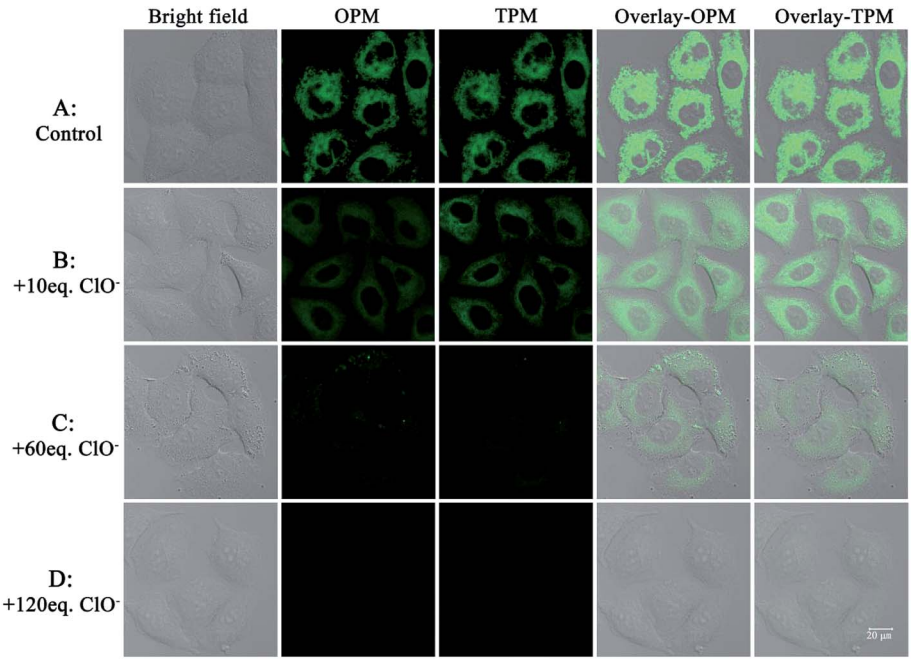

Fig. 5 One-photon and two-photon microscopy (OPM, TPM) confocal fluorescence images of A549 cells. Images of cells incubated with probe **1** (20 μM) for 30 min (control, (A)). Images of cells incubated with probe **1** for 30 min and subsequently with ClO^- (10 equiv., (B); 60 equiv., (C); 120 equiv., (D)). The probe was excited at 458 nm (OPM) or 810 nm (TPM). The emission was collected at 520 ± 30 nm. Overlay-OPM: overlay of bright field and OPM columns. Overlay-TPM: overlay of bright field and TPM columns.

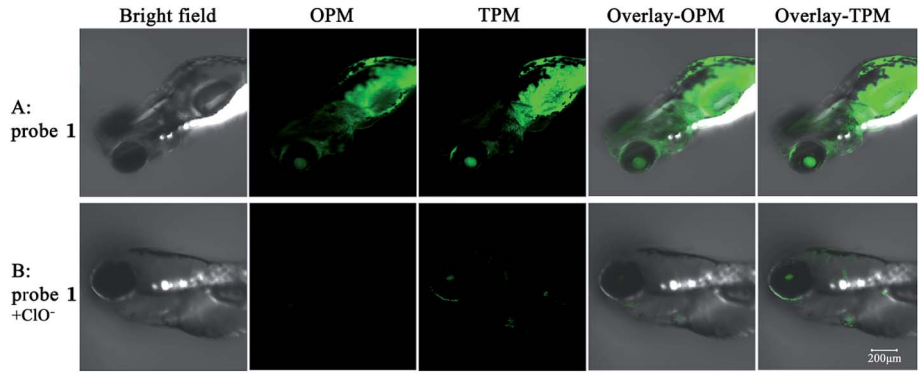

Fig. 6 Images of zebrafish larvae treated with 20 μM probe **1** in the absence and presence of 120 equiv. ClO^-. The probe was excited at 458 nm (OPM) or 810 nm (TPM). The emission was collected at 520 ± 30 nm. Overlay-OPM: overlay of the bright field and OPM columns. Overlay-TPM: overlay of the bright field and TPM columns.

fluorescence in the green channels by both one-photon and two-photon modes. Upon further incubation with 120 equiv. ClO^- for another 30 min, green fluorescence in all of the body of the zebrafish by both one-photon and two-photon imaging was almost completely quenched. The probe could be suitable for ClO^- detection in living zebrafish. Therefore, the probe has potential application of detecting ClO^- *in vivo* by fluorescence signal changes.

Conclusions

In conclusion, a coumarin Schiff's base-based probe selective for hypochlorite anion has been developed. The probe shows ratiometric fluorescence and remarkable fluorescence intensity change in response to ClO^- but not other common anions and some biologically related species. Moreover, this probe could be applied to detect ClO^- in living cells and zebrafish by both one- and two-photon microscopy imaging. The mechanism of the quick transition from green fluorescence to blue fluorescence in response to hypochlorite is attributed to nucleophilic addition followed by hydrolysis. With the characteristics of fast response rate, high selectivity, low cytotoxicity, good cell permeability and two-photon effect, we believe that the probe could have a lot of practical application in environmental and biological systems.

Experimental

Photophysical properties and response to hypochlorite anion

UV-vis absorption and fluorescence spectral titrations were carried out on a Shimadzu UV2550 spectrophotometer and a Horiba Fluoromax-4 fluorescence spectrometer, respectively. The solvent for titration experiments was phosphate buffer/MeOH (6 : 4, v/v, pH 7.4). The spectral changes were monitored with the addition of a solution of sodium hypochlorite (available chlorine content 5%) in deionized water as ClO^- source. Fluorescence quantum yield was obtained with coumarin 307 as ref. 32 by a previously published method.[33]

Cell culture conditions

A549 cells were maintained in Roswell Park Memorial Institute 1640 (RPMI 1640) medium containing 1% antibiotic solution, 10% FBS (fetal bovine serum), 100 U mL^{-1} penicillin and 100 μg mL^{-1} streptomycin. The A549 cells were cultured in an incubator with 95% air and 5% CO_2 at a constant temperature of 37 °C. A549 cells were obtained from the Experimental Animal Center of Sun Yat-Sen University (Guangzhou, PR China).

Cell viability assay

The cytotoxicity of the probe towards A549 cell lines was determined by methyl thiazolyl tetrazolium (MTT) assay.[34,35]

One- and two-photon cellular imaging

A549 cells were treated with 20 μM probe **1** in RPMI 1640 medium. After 30 min, RPMI 1640 medium was removed and washed with PBS buffer twice to remove excess probe **1**. Then A549 cells were further incubated with NaClO solution in PBS for 10 min.

One- and two-photon imaging of zebrafish

Zebrafish were obtained from the Experimental Animal Centre of Sun Yat-sen University (Guangzhou, PR China). All the experiments were approved by the Institutional Animal Care and Use Committee (IACUC) of Sun Yat-Sen University according to the requirements of the National guideline for the care and use of laboratory animals (PR China). The zebrafish were incubated in E3 medium[36] for 6 h and then 20 μM probe was added for another 1 h at 28 °C. The zebrafish were anesthetized with 1% chloral hydrate and subjected to luminescence imaging by confocal laser scanning microscopy. Other zebrafish were incubated with 20 μM probe for 1 h in E3 medium, and then 2.5 mM NaClO was added to treat for another 1 h at 28 °C. One- and two-photon imaging of zebrafish was carried out by a previously published method.[37]

Conflicts of interest

There are no conflicts to declare.

Acknowledgements

This work was supported by the National Natural Science Foundation of China (21672130, 21601065), and the Natural Science Foundation of Shandong Province (ZR2017MEM006), Colleges and Universities Science and Technology Foundation of Shandong Province (J16LA08).

References

1 X. Q. Chen, X. Z. Tian, I. Shin and J. Yoon, *Chem. Soc. Rev.*, 2011, **40**, 4783–4804.
2 H. X. Zhang, J. Liu, C. L. Liu, P. C. Yu, M. J. Sun, X. H. Yan, J. P. Guo and W. Guo, *Biomaterials*, 2017, **133**, 60–69.
3 H. D. Xiao, K. Xin, H. F. Dou, G. Yin, Y. W. Quan and R. Y. Wang, *Chem. Commun.*, 2015, **51**, 1442–1445.
4 A. Balamurugan and H.-i. Lee, *Macromolecules*, 2015, **48**, 3934–3940.
5 Q. L. Xu, K. A. Lee, S. Lee, K. M. Lee, W. J. Lee and J. Yoon, *J. Am. Chem. Soc.*, 2013, **135**, 9944–9949.
6 L. Wu, I. C. Wu, C. C. DuFort, M. A. Carlson, X. Wu, L. Chen, C. T. Kuo, Y. L. Qin, J. B. Yu, S. R. Hingorani and D. T. Chiu, *J. Am. Chem. Soc.*, 2017, **139**, 6911–6918.
7 K. Dou, Q. Fu, G. Chen, F. B. Yu, Y. X. Liu, Z. P. Cao, G. L. Li, X. E. Zhao, L. Xia, L. X. Chen, H. Wang and J. M. You, *Biomaterials*, 2017, **133**, 82–93.
8 L. B. Zang, C. S. Liang, Y. Wang, W. H. Bu, H. C. Sun and S. M. Jiang, *Sens. Actuators, B*, 2015, **211**, 164–169.
9 K. Y. Zhang, J. Zhang, Y. H. Liu, S. J. Liu, P. L. Zhang, Q. Zhao, Y. Tang and W. Huang, *Chem. Sci.*, 2015, **6**, 301–307.
10 X. H. Cheng, S. H. Qu, Z. C. Zhong and W. N. Li, *J. Fluoresc.*, 2017, **27**, 1427–1433.
11 L. S. Walekar, S. P. Pawar, A. H. Gore, V. D. Suryawanshi, S. S. Undare, P. V. Anbhule, S. R. Patil and G. B. Kolekar, *Colloids Surf., A*, 2016, **491**, 78–85.
12 Y. R. Zhang, Y. Liu, X. Feng and B. X. Zhao, *Sens. Actuators, B*, 2017, **240**, 18–36.
13 G. F. Wu, F. Zeng and S. Z. Wu, *Anal. Methods*, 2013, **5**, 5589–5596.
14 L. L. Long, Y. J. Wu, L. Wang, A. H. Gong, F. L. Hu and C. Zhang, *Chem. Commun.*, 2015, **51**, 10435–10438.
15 A. S. Murugan, N. Vidhyalakshmi, U. Rameshb and J. Annaraj, *J. Mater. Chem. B*, 2017, **5**, 3195–3200.
16 L. Chen, J. W. Ye, H. P. Wang, M. Pan, S. Y. Yin, Z. W. Wei, L. Y. Zhang, K. Wu, Y. N. Fan and C. Y. Su, *Nat. Commun.*, 2017, **8**, 15985.
17 K. M. Xiong, F. J. Huo, C. X. Yin, Y. Y. Chu, Y. T. Yang, J. B. Chao and A. M. Zheng, *Sens. Actuators, B*, 2016, **224**, 307–314.
18 J. F. Li, F. J. Huo and C. X. Yin, *RSC Adv.*, 2014, **4**, 44610–44613.
19 J. W. Li, C. X. Yin, F. J. Huo, K. M. Xiong, J. B. Chao and Y. B. Zhang, *Sens. Actuators, B*, 2016, **231**, 547–551.
20 B. C. Zhu, Y. H. Xu, W. Q. Liu, C. X. Shao, H. F. Wu, H. L. Jiang, B. Du and X. L. Zhang, *Sens. Actuators, B*, 2014, **191**, 473–478.
21 F. Y. Liu, Y. L. Gao, J. T. Wang and S. G. Sun, *Analyst*, 2014, **139**, 3324–3329.
22 Y. Xiao, R. Zhang, Z. Q. Ye, Z. C. Dai, H. Y. An and J. L. Yuan, *Anal. Chem.*, 2012, **84**, 10785–10792.
23 L. Yuan, W. Y. Lin, Y. N. Xie, B. Chen and J. Z. Song, *Chem.–Eur. J.*, 2012, **18**, 2700–2706.
24 R. Zhang, Z. Q. Ye, B. Song, Z. C. Dai, X. An and J. L. Yuan, *Inorg. Chem.*, 2013, **52**, 10325–10331.
25 M. G. Ren, B. B. Deng, J. Y. Wang, X. Q. Kong, Z. R. Liu, K. Zhou, L. W. He and W. Y. Lin, *Biosens. Bioelectron.*, 2016, **79**, 237–243.
26 D. X. Li, Y. Feng, J. Z. Lin, M. Chen, S. X. Wang, X. Wang, H. T. Sheng, Z. L. Shao, M. Z. Zhu and X. M. Meng, *Sens. Actuators, B*, 2016, **222**, 483–491.
27 X. M. Wang, X. H. Wang, Y. Feng, M. Z. Zhu, H. Yin, Q. X. Guo and X. M. Meng, *Dalton Trans.*, 2015, **44**, 6613–6619.
28 K. N. Wang, L. Ma, G. Q. Liu, D. X. Cao, R. F. Guan and Z. Q. Liu, *Dyes Pigm.*, 2016, **126**, 104–109.
29 P. Y. Ma, B. Zhang, Q. P. Diao, L. Li, Y. Sun, X. H. Wang and D. Q. Song, *Sens. Actuators, B*, 2016, **233**, 639–645.
30 H. J. Kim, C. H. Heo and H. M. Kim, *J. Am. Chem. Soc.*, 2013, **135**, 17969–17977.
31 C. Y. Li, M. X. Yu, Y. Sun, Y. Q. Wu, C. H. Huang and F. Y. Li, *J. Am. Chem. Soc.*, 2011, **133**, 11231–11239.
32 G. A. Reynolds and K. H. Drexhage, *Opt. Commun.*, 1975, **13**, 222–225.
33 J. N. Demas and G. A. Crosby, *J. Phys. Chem.*, 1971, **75**, 991–1024.
34 Y. Li, G. F. Liu, C. P. Tan, L. N. Ji and Z. W. Mao, *Metallomics*, 2014, **6**, 1460–1468.
35 L. He, C. P. Tan, R. R. Ye, Y. Z. Zhao, Y. H. Liu, Q. Zhao, L. N. Ji and Z. W. Mao, *Angew. Chem., Int. Ed.*, 2014, **53**, 12137–12141.
36 G. Y. Li, Q. Lin, L. L. Sun, C. S. Feng, P. Y. Zhang, B. Yu, Y. Chen, Y. Wen, H. Wang, L. N. Ji and H. Chao, *Biomaterials*, 2015, **53**, 285–295.
37 B. L. Dong, X. Z. Song, X. Q. Kong, C. Wang, Y. H. Tang, Y. Liu and W. Y. Lin, *Adv. Mater.*, 2016, **28**, 8755–8759.